ARTICLE TEMPLATE

Optimising structure in a networked Lanchester Model for Fires and Manoeuvre in Warfare

Alexander C. Kalloniatis[a], Keeley Hoek[b], Mathew Zuparic[a] and Markus Brede[c]

[a] Joint and Operations Analysis Division, Defence Science and Technology Group, Canberra, ACT, Australia; [b] Mathematical Sciences Institute, Australian National University, Canberra, Australia; [c] Agents, Interactions and Complexity Group, Department of Electronics and Computer Science, University of Southampton, Southampton, UK.

ABSTRACT
We present a generalisation of the classical Lanchester model for directed fire between two combat forces but now employing networks for the manoeuvre of Blue and Red forces, and the pattern of engagement between the two. The model therefore integrates fires between dispersed elements, as well as manoeuvre through an internal-to-each-side diffusive interaction. We explain the model with several simple examples, including cases where conservation laws hold. We then apply an optimisation approach where, for a fixed-in-structure adversary, we optimise the internal manoeuvre and external engagement structures where the trade-off between maximising damage on the adversary and minimising own-losses can be examined. In the space of combat outcomes this leads to a sequence of transitions from defeat to stalemate and then to victory for the force with optimised networks. Depending on the trade-off between destruction and self-preservation, the optimised networks develop a number of structures including the appearance of so-called sacrificial nodes, that may be interpreted as feints, manoeuvre hubs, and suppressive fires. We discuss these in light of Manoeuvre Warfare theory.

1. Introduction

In the age of high powered computers it has become accepted folklore that the days of understanding warfare through equation-based models are over. This is argued to be the case because of the multiplicity of factors influencing modern warfare, such as dispersed forces, networked Command and Control (C2), diverse rivals and stakeholders in conflicts, and technologies for Intelligence-Surveillance-Reconnaissance (ISR). In this paper we propose and explore a model that offers a platform to bring such factors together while still retaining the advantages of equation based approaches. At the heart of this remain the Lanchester equations for combat (Lanchester, 1916). For

---

CONTACT A. C. Kalloniatis. Email: alexander.kalloniatis@dst.defence.gov.au

directed fires these are

$$
\begin{aligned}
\dot{B}(t) &= \gamma_B B(t) - \kappa_R R(t) \\
\dot{R}(t) &= \gamma_R R(t) - \kappa_B B(t)
\end{aligned}
\tag{1}
$$

where $B(t), R(t)$ represent the total number of forces of Blue and Red at time t, γ_B, γ_R the rate of resupply, and κ_B, κ_R represent their respective kill-rates of the other. The κ are also variously referred to as fire-rates or fire-power or lethality, terms which we shall use interchangeably. The so-called 'undirected fire' version of these have $B(t)R(t)$ on the right-hand side of the equations. Proposed in 1916 by F.W. Lanchester, these simple equations have seen diverse uses beyond the original context of the statically arrayed massed fires of World War I. Such extensions will be reviewed below, but nascent is the incorporation of recent concepts such as as Network Centric Warfare (Alberts, Garstka and Stein, 1999), and realised in General Stanley McChrystal's strategy for battling the Taliban in Afghanistan "It takes a network to defeat a network" (McChrystal, 2011). Nevertheless, a fully networked version of the Lanchester model has not, to our knowledge, been written down.

In other dynamical systems, the network approach is well-developed, offering insights into various complex systems – biological, social and technological (Bornholdt and Schuster, 2003) – through numerical simulation and analytical approximation. The network paradigm has advanced to *multi-layer* networks (Boccaletti et al., 2014), where the connectivity within any layer and across layers may vary considerably. In warfare such layers may describe how forces are internally distributed, how they engage with the enemy, how C2 is arranged, and how ISR systems enable situation awareness. This paper takes initial steps towards capturing some of these using the multi-layer formalism.

We propose a form of the Lanchester equations whereby rival heterogeneous forces manoeuvre internal resources, and apply force against each other on external networks. We explore optimisation of these networks and observe emergent behaviours that may be interpreted through known manoeuvre warfare concepts.

We first review the literature on the Lanchester model, situating our formulation in recent variations of the model. We propose our networked Lanchester model and examine a small scale example to illustrate its dynamics. We then outline the optimisation and explore the trade-off between a force seeking to minimise its losses versus maximising its degradation of the adversary. In particular, we observe behaviours that may be interpreted as 'concentration', 'suppressive fire' and 'feints', concepts well-known in manoeuvre warfare. We show how some of these behaviours arise analytically exploiting the power of the Lanchester analytical framework. We then conclude, discuss these aspects in light of the literature on Manoeuvre Theory of warfare, and offer prospects for the future. An appendix provides analytical explanation for some of the numerical results and supplementary material presents an alternate constraint in the optimisation scenario.

2. Status of Lanchester combat modelling

Enhancements of the original Lanchester equations are many. As a description of the waxing and waning of two abstract entities, the equations may be interpreted more generally than mortal combat, for example in terms of network cyber-attack and defence (Liu et al., 2013). Mathematical generalisations include: general power law

$B^\alpha R^\beta$ forms for the right hand side (Epstein, 1997) and other nonlinear forms (Kim et al., 2017), stochastic diffusive models with advection (Protopopescu, Santoro and Dockery, 1989) and swarming effects (Keane, 2011) as partial differential equations, and game theory applications (Hohzaki and Higashio, 2016). These still only represent two homogeneous sets of forces arrayed against each other. In this era of joint or combined operations and multi-role platforms, the need for representing mixed-forces becomes acute. For such mixed-forces, numerous authors have proposed the (N, M) Lanchester problem of N Blue forces arrayed against M Red forces. Suppressing, at this stage, logistics/replenishment, this can be expressed through the system ($i = 1, \ldots, N; j = 1, \ldots, M$)

$$\dot{B}_i(t) = -\sum_{j=1}^{M} \mu(B)_{ij} R_j$$

$$\dot{R}_j(t) = -\sum_{i=1}^{N} \mu(R)_{ji} B_j, \tag{2}$$

where the μ capture the distribution of fire between units of Blue and Red respectively in a manner that tailors the rate to the adversary unit; for this reason some functional dependence of the μ on B or R is indicated. (Note that many authors use upper and lower indices according to attack and defence, which we will treat symmetrically).

Early such approaches are (Roberts and Connolly, 1992) on the $(2, 1)$ problem and (Colegrave and Hyde, 1993) on the $(2, 2)$ case who typically used time-independent $\mu(B)_{ij}, \mu(R)_{ij}$. It was pointed out in (Kaup et al., 2005) that such heterogeneous models cannot be interpreted in terms of the reality of combat; significant discontinuities in the redistribution of fire must be taken into account when units reach the value zero, when combat entities die. They proposed a model where the lethality depends on the attacker and the defender such that when one defender is destroyed the attacker may engage other targets.

These concerns have been furthered in a series of works authored solely or jointly by MacKay, starting with (MacKay, 2009) where analytic solubility could be gained by considering certain separable but dynamical forms $\mu_{ij}(t) = \kappa_i \mu_j(t)$, using weighted-ratios of one force element to the total weighted-sum of the force, for example $\mu_i(t) = \rho_i B_i(t)/\sum_j \rho_j B_j(t)$. These reflect that a commander may have a choice in how to distribute fire at the start of a battle but thereafter it evolves according to the proportion of units of a particular type. This was challenged by (Liu et al., 2012) who allowed for targets to change during battle as adversary units were eliminated. This also was questioned by MacKay, noting that in the fog-and-friction of war, such reallocation of targets may be unrealistic after the battle has begun (MacKay, 2012). We return to these points when we develop our model.

MacKay's formulations generate conserved quantities generalising the Lanchester square law for directed fire, $\kappa_R R(t)^2 - \kappa_B B(t)^2$ when $\gamma_B = \gamma_R = 0$ in Eqs.(1). This determines the victor based on initial conditions. All these authors recognise very well that these equations purport to describe battle of annihilation; quantities changing sign have no meaning. Within a 'kinetic effects' interpretation (as opposed to non-lethal, such as cyber (Liu et al., 2013)) the mixed forces models remain representations of unmitigated attrition, of "perfectly horrible" warfare (MacKay, 2009).

3. The networked Lanchester model

Readers will recognise a network structure in Eqs.(2): the μ_{ij} may be interpreted as weighted adjacency matrix elements describing the engagement interaction between the heterogeneous Blue and Red units. For $\mu_{ij} \in (1,0)$ we have a network of undirected links of nodes (i,j) that are connected, respectively unconnected. Though many authors seek to model 'networked forces' in Lanchester combat (Tang and Li, 2012), (Liu et al., 2013), none to our knowledge explicitly represent the network structure in the dynamics of the combat.

This offers an opportunity of overcoming one of the limitations of even the mixed Lanchester model, that through the course of battle a force may be dynamically reconfigured to reinforce weak units or exploit weaknesses of the adversary. This seeking to gain "advantageous position relative to the enemy" (Lind, 1985) is known as 'manoeuvre warfare', and is a further 'warfighting function' after attrition or 'fires'. 'Manoeuvre' captures the idea that success in the battlefield for forces with equally matched firepower unit for unit may be gained by not only providing more units, but through skillful manipulation of those units.

We propose for this the diffusive interaction for Blue force units $i, j = 1, \ldots, N$:

$$\dot{B}_i(t) = \sum_{j=1}^{N} \mathcal{B}_{ij} \left(\delta_i^{(B)}(t) B_i(t) - \delta_j^{(B)}(t) B_j(t) \right) \tag{3}$$

where $B_i(t) \in \mathbb{R}$, $\mathcal{B}_{ij}$ is a $(0,1)$ adjacency matrix and $\delta_i^{(B)}(t)$ represent possibly time-dependent weight factors between different Blue force elements. Such an approach has been used successfully for human population migration (Roman et al., 2017). It is trivially seen that for symmetric $\mathcal{B}_{ij}$

$$\sum_{i=1}^{N} \dot{B}_i(t) = 0 \tag{4}$$

as a consequence of the double sum becoming a difference under the sum of terms $k_i \delta_i B_i$, where we use the convention of $k_i = \sum_j \mathcal{B}_{ij} = \sum_j \mathcal{B}_{ji}$ for the degree of node i.

For the Red force, we introduce $R_i(t) \in \mathbb{R}$, and the corresponding internal adjacency matrix $\mathcal{R}_{lm}$ with nodes $l, m = 1, \ldots, M$ for Red agents. The networks $\mathcal{B}_{ij}$ and $\mathcal{R}_{lm}$ represent how a given distribution of resources $B_i(t) \geq 0$ and $R_l(t) \geq 0$ may *manoeuvre* dynamically through the course of battle; we distinguish this from a future extension with *logistics* networks that represent replenishment of the forces from outside the battle-space. Thus $\mathcal{B}_{ij}$ and $\mathcal{R}_{lm}$ are denoted as *manoeuvre* networks. Characteristic constants γ_B and γ_R determine the strength or time-scale of transfer of forces within the respective networks; these constants may be made node-dependent, not treated in this work.

Extending the network idea to the application of fires, we have *engagement* networks $\mathcal{E}_{il}^{(BR)}$ and $\mathcal{E}_{li}^{(RB)}$ (called μ_{ij} previously) representing the pattern of directed fires from one side to the other; these need not be symmetrical between Blue and Red. Correspondingly kill-rates κ_B and κ_R, as with Eq.(1), characterise the combat effectiveness of the respective forces. These, like γ_B, γ_R, may also be node or link dependent. Given the complexity already of this model, we consider homogeneous forces with uniform fire-power to understand the key impact of dynamical manoeuvre within each side's

forces. In the same spirit, we will use simplistic static engagement networks in contrast to (MacKay, 2009). Arguably, the ability to dynamically reallocate targets or the degree of fire-power may only be possible with improved ISR and a functioning C2 system able to integrate situation awareness into decision-making. Indeed, as we shall argue further below, sometimes in warfare strategies, are based on the adversary's over-estimation of the strength of some formations, or even that "dead" or "dummy" units may indeed be the mis-directed focus of attack.

Bringing these elements together gives an initial network generalisation of Eqs.(1):

$$\dot{B}_i = -\gamma_B \sum_j \mathcal{B}_{ij}(\delta_i^{(B)} B_i - \delta_j^{(B)} B_j) - \kappa_R \sum_m \mathcal{E}_{im}^{(RB)} R_m$$

$$\dot{R}_l = -\gamma_R \sum_m \mathcal{R}_{lm}(\delta_l^{(R)} R_l - \delta_m^{(R)} R_m) - \kappa_B \sum_j \mathcal{E}_{lj}^{(BR)} B_j. \tag{5}$$

This will not be the model's final form. The first terms in each set of equations are the manoeuvre contributions, where resource may be shifted through the respective networks according to relative strengths. The second set of terms are the engagement contributions but with predefined static distributions of fire.

Thus far, Eq.(5) describe a dynamics where the B_i, R_l may become negative: the equations need factors that forcing nodes to 'drop out' once resource levels reach zero. We may do this by Heaviside step functions $\Theta(x)$ or by a smeared form using the hyperbolic tangent function

$$\Theta_\epsilon(x) \equiv \frac{1}{2}(1 + \tanh(x/\epsilon)) \tag{6}$$

which for small ϵ approximates a step function at $x = 0$. In the same spirit, the diffusive transfer of resources to a weaker node should cease when that node has reached zero or a sufficiently low level ϑ. This may be achieved by using a shifted Heaviside function, $\Theta(x - \vartheta)$ but for simplicity we set $\vartheta = 0$. The third modification of the equations is to moderate the attrition term: in its form in Eq.(5) the entire resource of a node may be brought to bear on multiple nodes of the adversary without diminution. Thus it is more realistic to divide the attrition by the out-degree according to the engagement network,

$$k_i^{(RB)} \equiv \sum_m \mathcal{E}_{im}^{(RB)} \tag{7}$$

for the engagement of Red with Blue agent i, with the same for BR.

Thus the final form of the equations reads:

$$
\begin{aligned}
\dot{B}_i &= -\gamma_B \sum_j \mathcal{B}_{ij}(\delta_i^{(B)} B_i - \delta_j^{(B)} B_j)\Theta_\epsilon(B_i)\Theta_\epsilon(B_j) \\
&\quad -\kappa_R \sum_m \mathcal{E}_{im}^{(RB)} \frac{R_m}{k_i^{(RB)}}\Theta_\epsilon(B_i)\Theta_\epsilon(R_m) \\
\dot{R}_l &= -\gamma_R \sum_m \mathcal{R}_{lm}(\delta_l^{(R)} R_l - \delta_m^{(R)} R_m)\Theta_\epsilon(R_l)\Theta_\epsilon(R_m) \\
&\quad -\kappa_B \sum_j \mathcal{E}_{lj}^{(BR)} \frac{B_j}{k_l^{(BR)}}\Theta_\epsilon(R_l)\Theta_\epsilon(B_j).
\end{aligned}
\tag{8}
$$

For the weights δ we initially trialed constant values. Optimisation of the manoeuvre networks here generated *disconnected* graphs with isolated strong nodes and poorly connected weak nodes of commensurate initial conditions. The explanation for this is straightforward: connectivity here drains resource from strong nodes to weak which eventually die. Intuitively, channelling resource from strong to weak nodes should take into account their relative strengths to engaged adversaries. We therefore propose the following form, here for Blue's engagement with Red:

$$
\delta_i^{(B)} = \frac{1}{\sum_m \mathcal{E}_{im}^{(BR)} R_m + \epsilon},
\tag{9}
$$

with some regularisation parameter ϵ.

The choice of δ_i is a *warfighting heuristic*: not intrinsic to the model, it implements a principle for how a force seeks to achieve manoeuvre. While regularising divergences, ϵ also has physical meaning, noting that when $\sum_m \mathcal{E}_{im}^{(BR)} R_m$ vanishes, ϵ scales into the rate γ_R. Thus, ϵ represents a form of 'standing force' that a non-combatant node seeks to maintain: for small ϵ non-engaged nodes will give up resource rapidly to engaged partners; for large ϵ all nodes in the manoeuvre network will redistribute resource regardless of the state of engagements. In this work we will treat ϵ as infinitesimal. The model of Eqs.(8) offers a framework for testing the consequences of such heuristics. Our purpose then is to show that such a manoeuvre heuristic realises recognisable warfighting concepts, so the validity of the model will be determined *post hoc*.

We will be interested in equally resourced, fire-power matched but differently structured forces, so-called "near peer adversaries", as has become the focus of recent shifts in the US (US Army, 2017) and UK (Chuter, 2019) militaries, but without necessarily the 'massed force' paradigm (Cole, 2019). Thus, $B_i = R_i$ for engaged units (the distinction between indices i, j and l, m now becomes superfluous), or $\sum_j B_j = \sum_m R_m = T$. Given this, and because the model is linear we may divide through by the initial conditions $R_i(0) = B_i(0)$ or total force T. But from herein we consider $0 \leq B_i, R_l \leq 1$.

We will also set $\gamma_R = \gamma_B = 1$ and vary the lethality κ_R, κ_B. We will thus be examining the impact of differing lethalities of the two sides given different structures for manoeuvre and engagement *for fixed time-scale at which they are able to dynamically adapt* the allocation of their force.
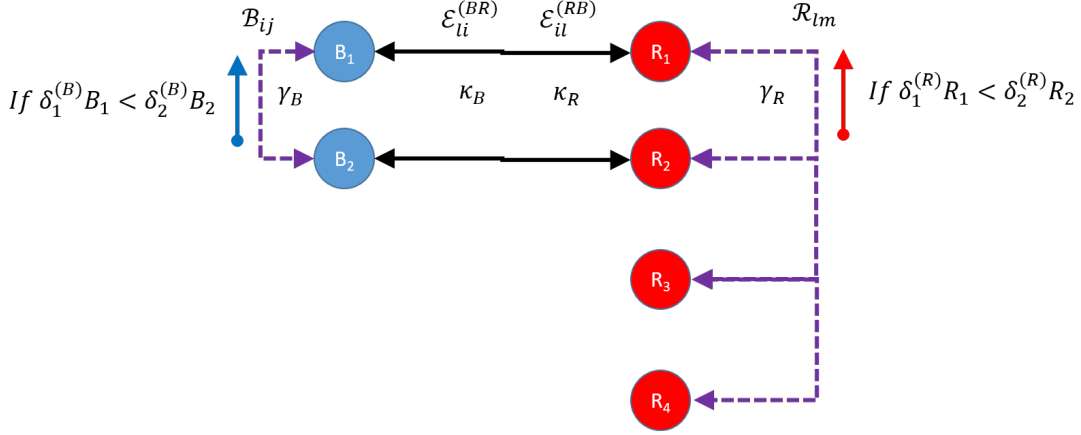
Figure 1. Illustration of the full model Eq.(8) with two Blue against four Red, where solid black lines indicated directed fire and purple dashed lines indicate resource sharing paths. Network quantities are labelled across the top and rates below the top row. The directions of flow, indicated by blue and red arrows, are governed by the conditions involving the δ; if the direction of the inequalities reverses so too does the direction flow.

4. Simple case study

To illustrate the key dynamics of the model we consider an engagement of two Blue units engaged against four Red units, where the latter use a manoeuvre network to draw reserves as defined in Eqs.(8,9). We will consider a number of ways of determining where manoeuvre provides advantage:

(1) initially equally matched adversaries, $B_i(0) = R_i(0) = 1/2$ for $i = 1, 2$ but with Red having varied reserves in $R_3(0) = R_4(0) = f_R/2$, so that $\sum_j B_j(0) = 1, \sum_m R_m(0) = 1 + f_R$;

(2) initially mismatched adversaries, $B_i(0) = 1/2, R_i(0) = f_R/2$ for $i = 1, 2$, but equal total, $\sum_j B_j(0) = \sum_m R_m(0) = 1$ so that $R_3(0) = R_4(0) = (1 - f_R)/2$ or zero if $f_R > 1$; and

(3) initially mismatched adversaries, but where Red has extra reserves it can call upon, namely $B_i(0) = 0.5, R_i(0) = f_R/2$ for $i = 1, 2$, as well as $R_l(0) = f_R/2$ for $l = 3, 4$ so that $\sum_j B_j(0) = 1, \sum_m R_m(0) = 2f_R$.

With the Blue kill-rate fixed at $\kappa_B = 1$, and equal manoeuvre rates $\gamma_R = \gamma_B$ we vary both the Red kill-rate κ_R and the fraction of the force available to Red. We focus first on case (3) for $\kappa_R < \kappa_B$ where Red has the most extreme initial disadvantage. How can Red's ability to manoeuvre spare resources provide advantage?

In Fig.2 are the profiles for the units as functions of time for the case of $f_R = 0.8$ and two marginally different values of $\kappa_R = 0.91, 0.92$ both less than $\kappa_B = 1$. Recall for case (3) the total resources available initially for Red are 1.6 but each Red combat unit begins with only 0.4 compared to Blue's 0.5. We also show the mean initial resource per unit, black for Blue and grey for Red so that Red is on average less resourced than Blue.

For the lower value of κ_R (left-hand panel), Blue's combat units maintain their initial advantage; the dashed and dotted red lines indicate Red reserves are offering resource to their combat partners, but too slowly, given the combat units' insufficient fire-power, to save the day. When the Red combat units have expired, their reserve counterparts stabilise as the combat has finished. Blue has won in terms of the combat
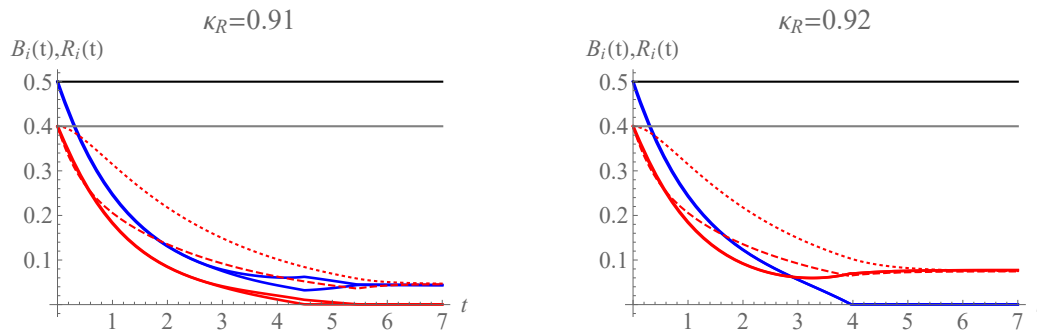
Figure 2. Case of two Blue against four Red dynamics for two different Red kill-rates, where Blue and Red solid lines represent engaged units and Blue and Red dashed/dotted lines represent supporting units. Black and gray represent the mean force per unit of Blue and Red respectively.

dynamics; the remaining Red units are unable to transfer any more resource into the fight.

With a small increase of fire rate by Red, this situation is reversed. In the right hand plot of Fig.2 Red is able to manoeuvre resources into the fight with Blue, and Red combat units are able to degrade Blue sufficiently, to enable Red to defeat Blue. After Blue's expiry, Red reserve units continue to share resource with combat units until they equalise and stabilise.

There is thus a balance between reserve capacity, fire power and manoeuvering rate enabling a set of combat units to defeat a unit-for-unit superior force.

Within the same model we explore the critical value of Red fire power, denoted κ_R^*, at which Red is able to defeat Blue for the different cases (1)-(3). To this end we numerically solve for sufficient time until one or the other combat force is degraded to zero for different κ_R, f_R and for the three cases of reserve supply. This is shown in Fig.3. In the plot we overlay a grey region where Red has weaker fire power and initial combat unit strength compared to Blue. In other words, curves that cross into the grey region show where Red genuinely gains advantage significantly because of its manoeuvre capability rather than numerical or weapon strength.

For the second case with equal total resource for both forces at the outset (dotted curve), f_R must exceed the value one for Red to achieve advantage with lesser fire-power. In other words, each Red combatant unit requires more than half the initial resource of the Blue combatants. Thus with the same total initial resource and lesser fire-power and initial strength, the Red force is able to defeat Blue through the manoeuvre of resource through its network. However, with even more total initial resource, it is possible for Red to achieve victory with even lower fire-power and initial resource for its combat units, as seen in the solid and dashed curves for values inside the grey region. We see then that the manoeuvre capability provides advantage over and above pure fire-power and strength.

5.   Optimal structures for manoeuvre and engagement

We now amplify the scale of forces represented in the model, and focus on how network heterogeneity develops to provide advantage to one side even with less raw fire-power than the adversary. We will be interested in the heterogeneity that emerges according
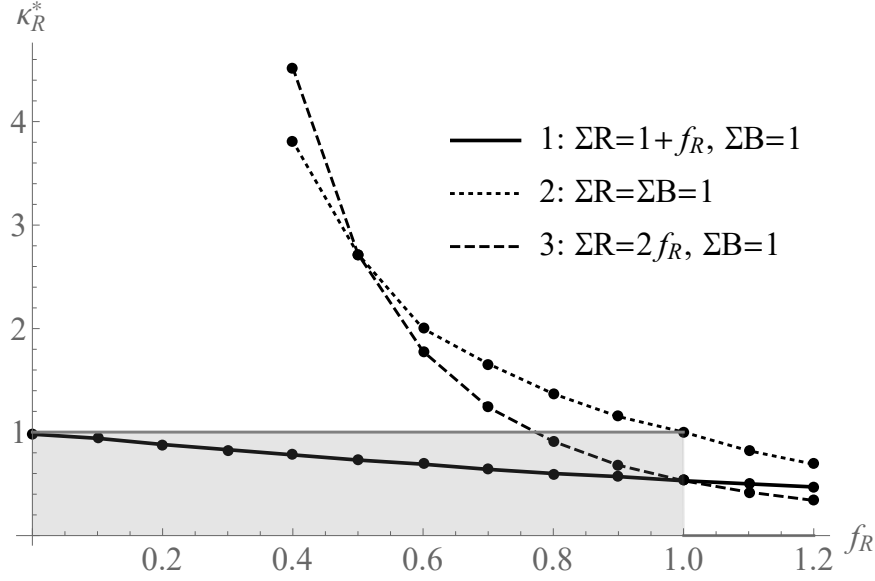
Figure 3. The critical value of κ_R at which for a value of f_R Red defeats Blue for the three different cases. With the grey region we indicate where Red gains advantage with lesser fire power and initial resource for its combat units.

to the balance of priorities of an optimal force.

5.1. *Network optimisation*

We consider optimisation of battle outcomes for one side, here chosen as Red. We presume that Red's decision makers are interested in overall outcomes in which certain trade-offs $U_R(\lambda)$ between their own remaining forces $R(t) = \sum_i R_i(t)/N$ and the number of destroyed and remaining opponents $B(t) = \sum_i B_i(t)/N$ are optimised; here $N = \sum_i R_i(0) = \sum_i B_i(0)$ since all $B_i(0), R_i(0) = 1, i = 1, \ldots, N$. Because of equal initial forces we cease distinguishing between indices $(i, j, k, l) \in (1, \ldots, N)$. We quantify utility for Red by

$$U_R(\lambda) = \lambda R + (1 - \lambda)(B(0) - B), \tag{10}$$

where $B(0)$ gives the initial average force of Blue and λ measures a trade-off between an interest in preserving their own forces ('defence') and destroying the adversaries' forces ('offence'). Since we do not include resupply terms here this quantity will be non-negative.

The optimisation scheme is based on stochastic hill-climbing, to maximise U_R. In more detail:

(1) Start with some initial engagement and manoeuvre networks R_{ij}, B_{ij} and $\mathcal{E}_{ij}^{RB} = \mathcal{E}_{ji}^{BR}$, based on Erdos-Renyi random graphs, which are built by randomly assigning links between nodes according to a uniform probability; here we use average degree of the network $k = 4$. The combination of manoeuvre and engagement networks for one side we refer to as a 'configuration'.

(2) Perform a random rewiring of Red's configurations by, either, with some probability p rewiring Red's manoeuvre network R_{ij} or, with probability $1-p$, rewiring

of Red's engagement network $\mathcal{E}_{ij}^{RB}$. For these modifications of the manoeuvre network, we pick a randomly selected link and move it to a randomly selected link vacancy, thus preserving the average degree of the manoeuvre network. Similarly, for modifications in the engagement network, we select one engagement link uniformly at random and move it to a randomly selected link vacancy in the engagement network. Additionally, we also consider additions of new engagement links to randomly selected engagement network link vacancies or removal of randomly selected engagement links, such that Red can optimise the number of engagements it wants to participate in.

(3) For this modified structure we then numerically integrate the respective network Lanchester system Eqs.(8) to determine stationary force concentrations and evaluate Red's utility $U_R(\lambda)$. New configurations are accepted if the stochastic modification resulted in an improvement in Red's utility, otherwise we reject the modification. In the first case, we keep the modified configuration and repeat (2). In the second case, we restore the previous battle structure before repeating step (2).

To integrate the equations we use fourth order Runge-Kutta with time-step $\delta t = 0.01$. Optimisation steps are repeated in the order of 10^5 times, ensuring near-convergence to a final configuration. We repeat the procedure for a fixed number of different random initial conditions, and check final configurations to ensure the robustness of our findings presented below. We have also attempted simulated annealing to avoid trapping in local minima, however such localised methods did not result in significant improvements compared to the method outlined here. One optimisation run of these 10^5 iterations takes approximately 2 hours, but most of our results below have been averaged over 20 independent runs, resulting in a simulation time of approximately 2 days for one choice of parameters.

Now we scrutinise the optimisation outcomes for a system with numbers of nodes $N_R = N_B = 50$, numbers of manoeuvre links $L_R = L_B = 100$, and numbers of engagement links $L_{RB} = 10$, and rates $\kappa_R = 0.5, \kappa_B = 1$ (thus Red is inferior to Blue in fire-power), and initial conditions $R_i = B_i = 1$. The Red force optimises both its manoeuvre network and the engagement. This scenario will remain the focus for the remainder of the paper. Fig.4 shows results for different values of λ exploring the offence-defence trade-offs. The first row has $\lambda = 0.2$, for emphasis on offence, the middle $\lambda = 0.5$, and the bottom row $\lambda = 0.9$, with emphasis on defence. The left column shows the density of surviving agents for each side and the value of the trade-off utility function as a function of the number of iterations of the optimisation process; the right column shows a typical network diagram with Blue and Red coloured manoeuvre networks at the end of the optimisation and green the symmetric engagement network; and the panels in Fig. 5 shows the surviving densities for networks optimized at $\kappa_R = 0.5$ and $\kappa_B = 1$ as a function of Red's and Blue's lethalities.

In the first column we observe the (approximate) plateauing of the curves showing equilibration of the optimisation, with the utility reaching a maximum value. We see the intuitive behaviour that, as λ increases with more emphasis on self-preservation, the equilibrium value of Blue ceases to be close to zero (panel (a)) but to a value of approximately 0.9 (panel (c)), though still less than the optimising Red force which suffers only very small losses.

In the networks in the right column (panels (d-f)) we show the structure at equilibrium and indicate the resulting force strength at each node by its size. The difference in structure for different λ is noteworthy. For low and intermediate λ we see a concentra-
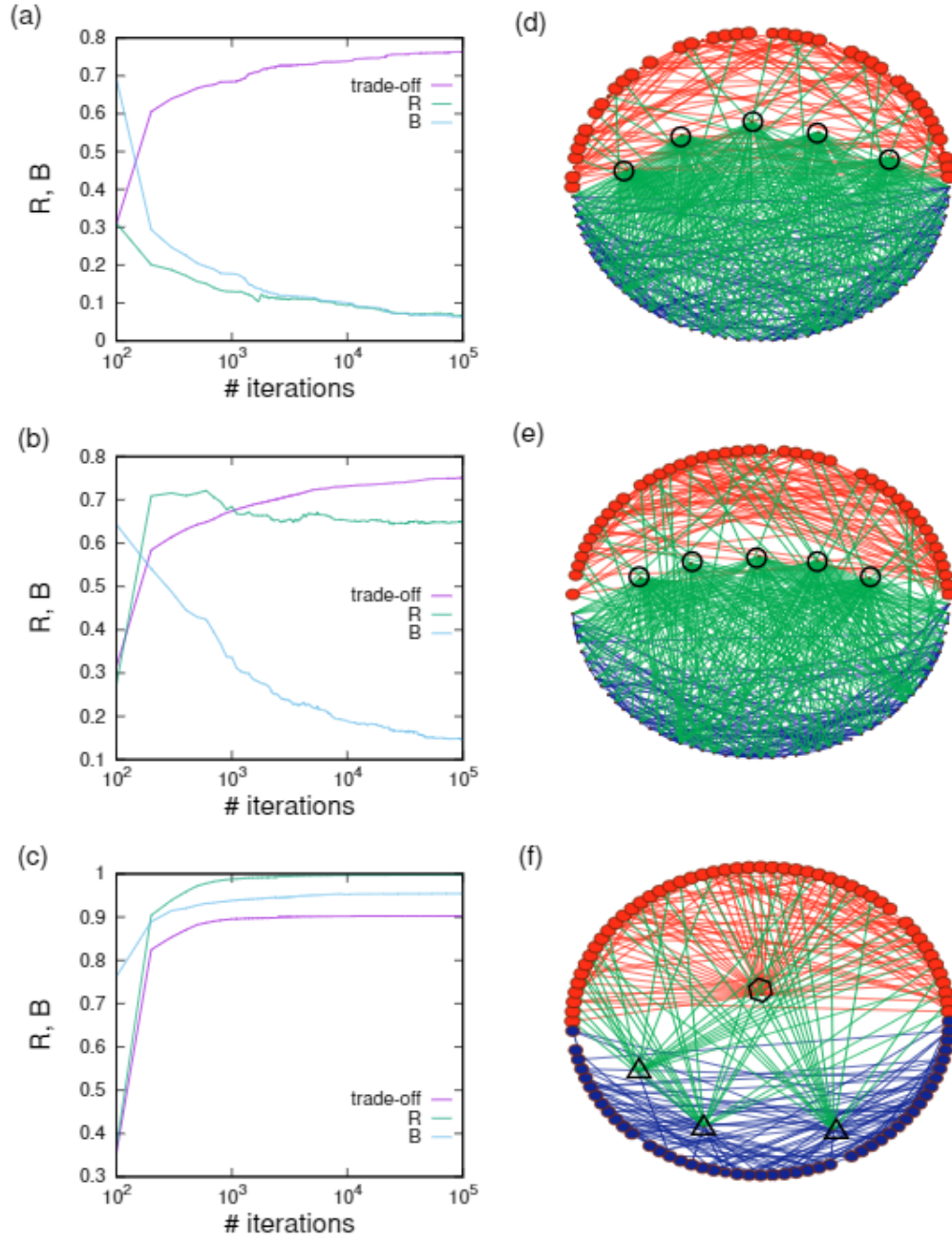
Figure 4. Evolution of stationary values of forces and trade-off utility function optimization for (a,d) low ($\lambda = 0.2$), (b,e) intermediate ($\lambda = 0.5$), and (c,f) large trade-off parameter λ ($\lambda = 0.9$). Trajectories are averaged over 20 independent runs. On the right, example networks at equilibrium after 10^5 optimisation iterations for (d) low, (e) intermediate, and (f) large λ as above. Red force nodes drawn in red, Blue force nodes in blue. Connections in the manoeuvre networks of Red and Blue forces in red or blue. Engagements are drawn in green. Nodes surrounded by a black circle indicate red sacrificial nodes, blue nodes in a triangle denote blue nodes at which Red's attack is focused. The red node in a diamond in (f) indicates a manoeuvre hub. In all cases the system size is $N_R = N_B = 50$, $L_R = L_B = 100$, $\kappa_R = 0.5, \kappa_B = 1$, and initial conditions $R_i = B_i = 1$.
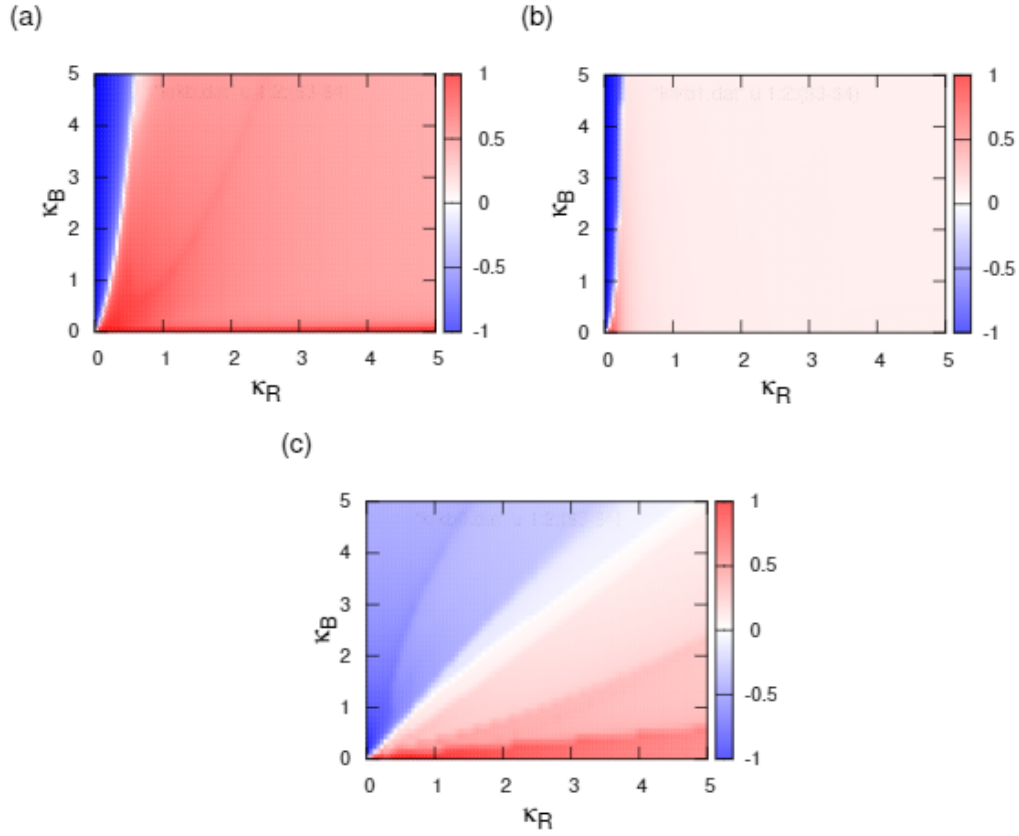
Figure 5. Heat map of differences between normalised stationary Red and Blue forces vs. lethalities κ_R and κ_B for the best configuration found for networks optimized for $\kappa_R = 0.5, \kappa_B = 1$ and (a) $\lambda = 0.5$ and (b) $\lambda = 0.9$. Panel (c) shows the heatmap for a random Blue and Red network with the numbers of links in the manoeuvre and engagement networks consistent with the optimised networks of Red. Red colours indicate regimes of larger Red surviving forces and Blue colours regimes of larger Blue surviving forces. In all cases the system size is $N_R = N_B = 50$, $L_R = L_B = 100$, $\kappa_R = 0.5, \kappa_B = 1$, and initial conditions $R_i = B_i = 1$.

tion of Red nodes that are multiply engaged with Blue, highlighted by a black circle. Significantly, as closer inspection shows, these are very weak nodes. These multiply engaged nodes may be termed 'sacrificial attackers', namely nodes attack many adversary nodes simultaneously. On the other hand these same nodes have few manoeuvre (red) links within their force, so that they are relatively unsupported. In this sense, they are sacrificed – many concurrent attacks with no local support so that they are allowed to drain of resource. We also observe at small λ in panel (d) an absence of Red hubs for manoeuvre, with a hint of clustering of Red nodes for $\lambda = 0.5$ in panel (e). Thus Red's emphasis on Blue's destruction manifests as little internal structure for its manoeuvre but a significant structure in the formation of sacrificial hubs. At high λ, with survival more significant in the utility function, a manoeuvre hub becomes more prominent in panel (f), highlighted by a black diamond. As can be seen, this node does not attack Blue. The large Red nodes on the ring boundary attack, but accumulate in different groups onto a few Blue targets, indicated by black triangles. Evidently, attacks are focused on a few Blue nodes which are quickly extinguished. These behaviours are a key insight from this approach to which we return later.

The panels of Fig. 5 shows the lethality dependence of the difference in the surviving densities for networks optimised at κ_R and $\lambda = 0.5, 0.9$ (note that the heatmap for $\lambda = 0.2$ is similar to that for $\lambda = 0.5$ and hence omitted), and then run simulations across different values of κ_R and κ_B. Such 'battle outcome' heatmaps represent a continuum of scenarios within the broad case of near-peer adversaries. As a reference case, panel (i) corresponds to random networks that are different instances of the same probability distribution. It is obvious that a region of larger surviving Blue forces is separated from a region of larger surviving Red forces by the diagonal line $\kappa_R = \kappa_B$. Hence, given random structure of engagement and manoeuvre networks, the force with larger lethality 'wins' and – visualised by more intense hues of the respective colours– victories are the more expressed the larger the distance to the diagonal line.

This scenario is dramatically altered for the optimised networks. In panel (a) we see the heatmap for a network optimised for $\lambda = 0.5$. It is now obvious that optimisation has dramatically reduced the area in parameter space that corresponds to Blue victories. Red victories typically correspond to a dark Red hue; as we have seen in Fig. 4(b,e), Red tends to win by eliminating the Blue force. Similarly, in panel (c) a heatmap for a configuration optimised for $\lambda = 0.9$ is shown. Inspecting panel (c) a further reduction in the Blue area is apparent: Blue wins are now restricted to a very small area of parameter space in which Blue has much larger lethality than Red. However, as a trade-off, the Red victory becomes coloured in a less intense red. Here Red is no longer able to eliminate most Blue but wins by preserving most of its force and destroying a small proportion of Blue (see also Fig. 4(c,f)).

Analysis of optimisation results for particular parameter configurations above hints to the existence of different regimes for optimal configurations. In the next section we proceed with a more systematic analysis of the dependence of properties of optimal configurations on the trade-off parameter λ.

5.2.   *Tradeoffs in optimal networks*

Now we study the dependence of the behaviours in optimised networks against the trade-off parameter λ. Here, for every value of λ we run the optimisation and take the five best configurations and average properties over these. We plot in Fig.6 the dependence of λ of averages of a range of quantities - the utility, numbers of evolved

links, numbers of sacrificers (as discussed above), the numbers of attacked nodes, and network degrees of various types. Note that Red wins in every case - as the optimised force - but the λ dependence of these quantities reveals different properties for Red to achieve its optimal performance.

Firstly, the utility function in panel (a) shows a steady decrease as λ increases until approximately $\lambda = 0.7$ at which point it begins to increase again. Thus as the two objectives - destruction of the adversary and survival of own forces - compete with each other the overall utility available decreases. We see distinct 'offensive' and 'defensive' phases which swap at $\lambda = 0.7$, and diminishing utility in the intermediate regime; 'pure' offence or defence objectives ($\lambda = 0$ and $\lambda = 1$ respectively) have higher utilities. We emphasise that 'defence' here always involves offence as fire is continuous, but the degree of seeking to preserve forces at the same time. This same point of transition, $\lambda = 0.7$, manifests in all the other measures. In the surviving forces in panel (b) we see it in a transition from complete Blue destruction in the offensive phase (it is Red that is optimised) to a coexistence of Blue and Red for $\lambda > 0.7$.

In panel (c) we compute the number of sacrificer nodes identified as those with no manoeuvre links with their own force but solely engaged with a sufficiently large number of adversary nodes. We choose $k = 10$ as the threshold. We observe three phases: a slight decrease for low λ, a plateau and then significant drop at high λ, again at the threshold value of $\lambda = 0.7$. In other words, sacrificial nodes are a significant structure in the optimal networks in the offensive phase.

The number of links per node in the evolved engagement networks, denoted l_{RB}, is shown in panel (d). Recall that the seed networks start with $L_{RB} = 10$ total number of links and 50 nodes, so l_{RB}, the ratio, may change through iterations of the optimisation. The plot in (d) exhibits several changes with increasing λ, though the transition at $\lambda = 0.7$ is also evident. Again, as the emphasis shifts from offence to defence there is a drop in the number of optimal engagement links. This transition is sharper in the fraction of attacked Blue nodes in panel (e): Red goes from attacking the entire Blue force in the offensive phase, to very few at the critical value of λ. In panel (f) we show the number of attacks on attacked Blue nodes, in other words the number of Red force agents that *simultaneously* attack a Blue node

This goes from a steady value of approximately $5 \leq k_{RB} \leq 10$ to an order of magnitude larger at the critical value of λ. In other words, as utility shifts in emphasis to self-preservation, Red must concentrate rather than disperse its engagement and thus chooses to engage very few Blue nodes (as seen in (e)) but with overwhelming force. A similar result is seen in panel (g) in the maximum degree of manoeuvre nodes in Red. These nodes of high degree are the manoeuvre hubs observed in the network diagrams of Fig.4.

To address the question whether Red attacks well supported or unsupported Blue nodes, in panels (h) and (i) we examine the overlap between manoeuvre and engagement in the force elements. Specifically, we measure the average manoeuvre degree of attacked Blue nodes (panel (h)) and the average degree of an attacking Red node (panel (i)).

Panel (h) shows how Red targets the manoeuvre network of Blue: up to the critical value of λ almost all Blue nodes are attacked and hence the average manoeuvre degree of *attacked* Blue corresponds to the average manoeuvre degree $k = 4$, after which it drops, though the error bars here are quite large. In the network diagram of Fig.4(f) we see such overwhelming attacks in the green links from multiple Red nodes on to three separate single Blue nodes inside the ring. The left-most one is evidently a poorly supported Blue node, while the right-most node appears to have a number of Blue

manoeuvre links feeding into it. Given that Blue remains an Erdos-Renyi network (it has not been subject to optimisation) we cannot speak here of a corresponding manoeuvre hub for Blue. So, for this form of structure, statistically in the defensive phase Red targets poorly supported Blue nodes.

In panel (i) we see the coincidence in Red of manoeuvre links that are attacking Blue, and see a drop at the critical λ, again with some noise. In the defensive phase Red tends to attack with nodes of low manoeuvre degree, but resources tend to be funnelled into these nodes from hub nodes in the Red manoeuvre network.

We see overall a consistent pattern that matches intuition, on the one hand, but is non-trivial in other respects: the offensive phase persists beyond the trade-off point of $\lambda = 0.5$, there is a pattern of sacrificial nodes appearing in the intermediate region, and manoeuvre hubs developing in the defensive regime. In the Appendix we show analytically how this phenomenon occurs in the model.

In the supplement we consider the case where the number of attacks may be constrained, arguably a more realistic scenario in warfare, and find similar behaviours to those described here except that in the offensive phase we find Red concentrating attacks to suppress the Blue force capacity to manoeuvre resources.

5.3. *Network structure dependence on Red fire-power*

Thus far we have fixed the fire-power, or lethality, of Red to a discrete set of values. We now examine the properties of optimised networks for varying Red lethality.

For this purpose we focus on the offensive regime and fix a trade-off parameter of $\lambda = 0.5$ (and $\kappa_B = 1$). We then optimise networks for varying values of κ_R and investigate their properties.

These results are shown in the various panels of Fig.7. In panel (a) we see the surviving densities of the two forces with the result that Red is superior for all κ_R but with a sharp increase between $0.3 \leq \kappa_R \leq 0.5$, and then a plateau for larger κ_R. Thus, given the trade-off between destruction of the adversary and self-preservation at this value of λ, there are diminishing returns for Red increasing its lethality beyond $\kappa_R = 0.5$. There is a corresponding flattening of Blue's curve at large κ_R. We superimpose on these plots the results for the original random Blue and Red graphs which seeded the optimisation procedure with the clear result that Red only overcomes Blue when it has the same lethality in the absence of optimal networks. Thus the optimisation for Red genuinely improves its performance across all values of κ_R compared to the initial seed configurations.

In (b) we show the number of attacks per node of Blue, namely the degree of Blue nodes in the engagement network. This evidently linearly increases with κ_R. A more powerful Red force will carry out more attacks than a less powerful Red force.

In (c) we give the average degree of manoeuvre nodes in Blue that are attacked by Red which shows a linear increase then at $\kappa_R = 1$ flattening to the average degree of the overall Blue manoeuvre network, $k = 4$. For low lethality Red cannot overwhelm the entire Blue force. Thus, in this regime Red focuses its attack on selected Blue nodes which are precisely those which are least supported by Blue's manoeuvre network. For increasing lethality Red then targets most Blue nodes, thus explaining the plateau.

Finally, (d) reveals how much of Red's network is 'dual-purpose', manoeuvre and engagement, by computing the manoeuvre degree of Red nodes that also attack Blue. The result is that at $\kappa_R \approx 1$ there is again, a transition: for low fire-power there are high-degree Red manoeuvre hubs that also engage Blue while at high fire-power these
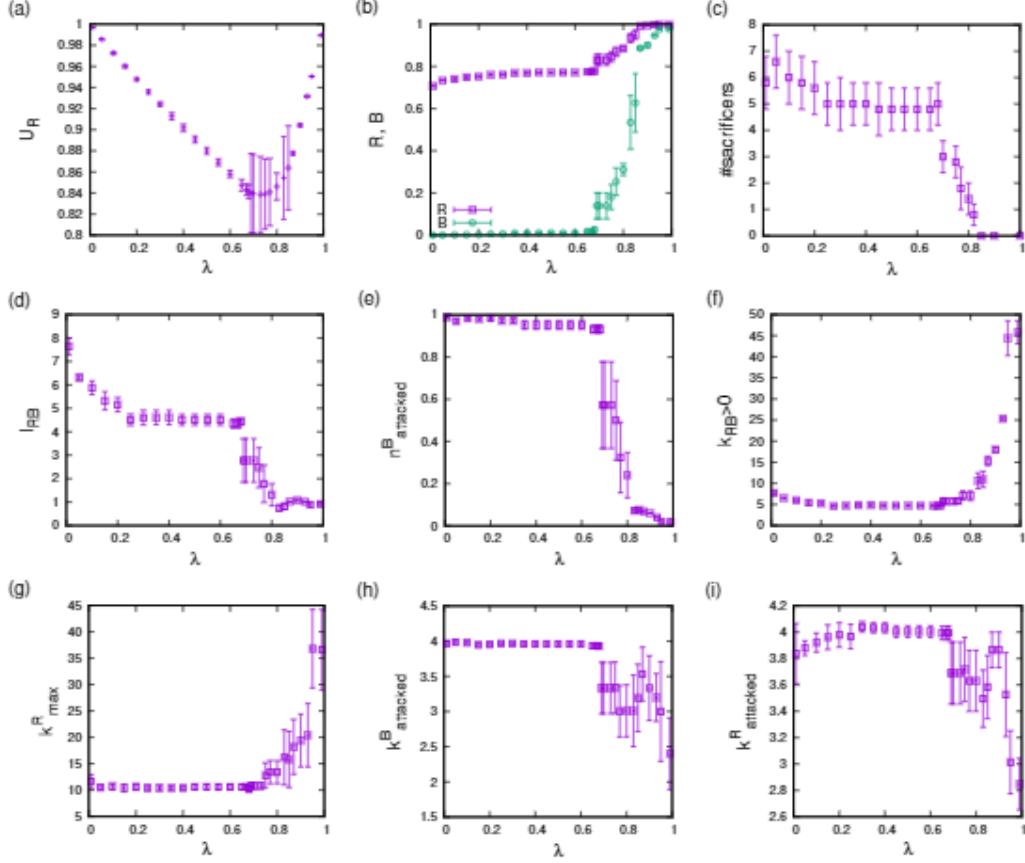
Figure 6. Dependence of properties of the optimised configurations on the trade-off parameter λ when optimising Red's utility $U_R = \lambda R + (1 - \lambda)(1 - B)$ (i.e. for $\lambda = 0$ R is only interested in extinguishing B whereas for $\lambda = 1$ force R is only interested in force preservation.) (a) Utility, (b) remaining stationary forces. (c) the number of sacrificial nodes, namely nodes with no input in the manoeuvre network but engagement degree $k > 10$, (d) evolved number of links per node (attacks), (e) fraction of attacked B nodes, (f) average number of attacks on attacked B-nodes, (g) evolved max. degree of R nodes in R's manoeuvre network (note that the avg. maximum degree for a random network with the same number of connections is 8.9 ± 0.5), (h) avg. degree in manoeuvre network of B nodes that are attacked by R, (i) avg. degree in manoeuvre network of R nodes that are attacking nodes of B. System of size $N_R = N_B = 50$, $L_R = L_B = 100$, $\kappa_R = 0.5, \kappa_B = 1$ (note that R is inferior to B), and initial conditions $R_i = B_i = 1$. Data points represent averages over the five best optimised configurations found for the respective value of λ, if not otherwise indicated error bars are about the size of the symbols. Force R optimises both its manoeuvre and engagement networks.
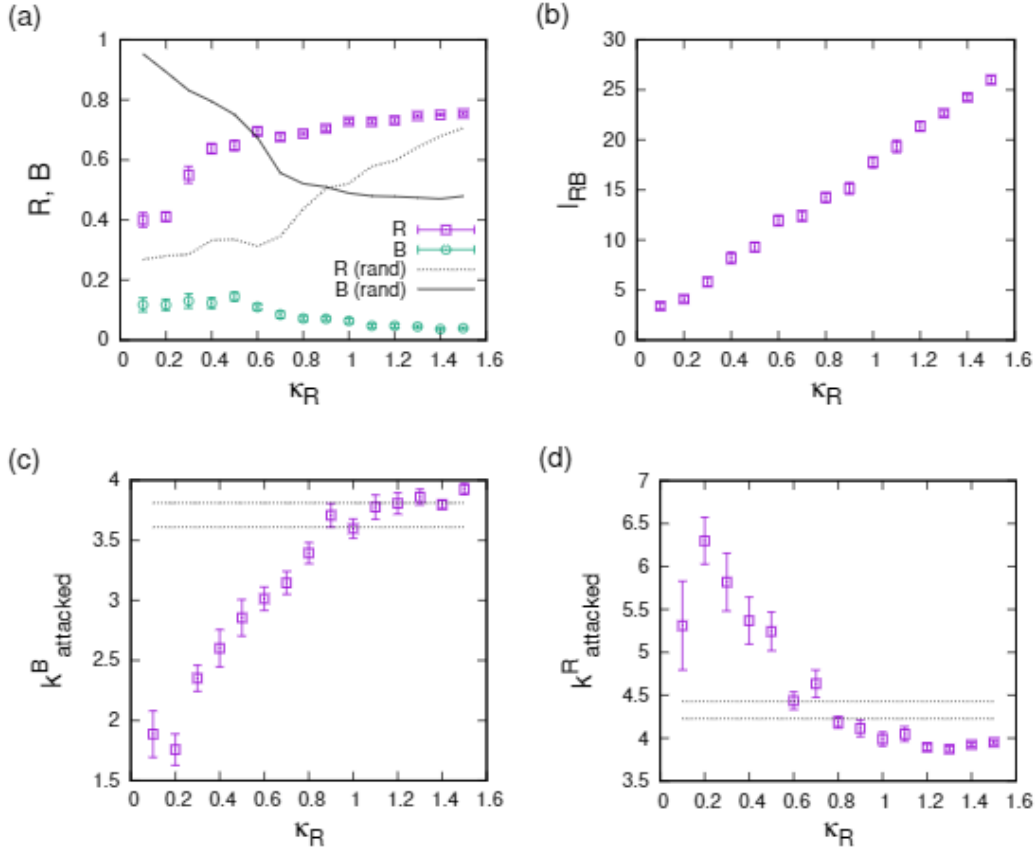
16

Figure 7. Outcomes for varying strength κ_R of Red when manoeuvre and engagement networks are optimised for $\lambda = 0.5$. (a) optimised stationary forces (solid lines give averages for a random networks that were used as seeds for the optimisation for comparison). (b) Avg. number of B nodes under attack from R. (c) avg. degree in the manoeuvre network B of B nodes that are attacked by R. (d) degree in the manoeuvre network of R of R nodes that attack B. In (c) and (d) the dotted lines indicate expectations (plus/minus one standard deviation) for random attacks calculated from the (random) networks that were used to seed the optimisation. Data points represent averages over 20 optimisation runs.

dual-purpose hubs have disappeared. In light of the evidence for Red manoeuvre hubs in the networks of Fig.4, this suggests that at high fire-power the hubs become more specialised, purely manoeuvre or attack.

In (c) and (d) we also give in the dotted lines the expectation within one standard deviation of the result using the original random networks that seeded the optimisation. We see that the results are constant in κ_R, so that there is nothing distinguishing in the networks between manoeuvre and engagement nodes in the overall combat outcome, due to the uniform random nature of the Erdos-Renyi graph. In other words, the optimisation is generating specialised roles in the manoeuvre and engagement structure of Red that are different at the various values of lethality.

In summary to the analyses thus far, we conclude that optimising with higher fire-power, when offence and defence are similarly weighted in utility, gives diminishing returns. An optimised Red force structure with lesser lethality than Blue is able to achieve victory through dual-purposing manoeuvre and attack hubs. In the supplement, when the optimal force is constrained in the number of targets it may engage, in the offensive phase it focuses on the adversary ability to manoeuvre its own forces.

We shall discuss later the extent to which these results resonate with ideas in Manoeuvre Warfare.

5.4. *Battle-outcome heatmaps for optimised networks*

We now take exemplar optimal networks and scan across the parameters for the Red force, γ_R, κ_R, to examine the regions where that force has advantage over Blue. This type of analysis would be typical as an application of our model for trade-offs in investment over technology that either enhances fire-power or manoeuverability of a force but also where optimisation of structure, both for manoeuvre and engagement, is a consideration.

We consider again forces of equal size $N = 50$ and number of manoeuvre links $L_R = L_B = 100$ and optimise the Red force at $\kappa_R = 0.5, \gamma_R = 1$ against a Blue force with $\kappa_B = 1, \gamma_B = 1$. We examine two cases, with trade-off parameter $\lambda = 0.5$ for the offensive phase and $\lambda = 0.9$ for the defensive phase. We then solve the system to determine steady-state densities of force at $\kappa_B = 3$, for a *more powerful adversary than the one for which Red has optimised*. In Fig.8 we plot battle-outcome heatmaps, similar to those in Figs.4 (g-i) but for Red's variable choices, γ_R, κ_R.

We note the following key features in these results in Fig.8. Firstly, in all cases of optimised network there is a threshold lethality required before Red has an advantage over Blue. In panel (a), this threshold is close to that used for the optimisation, $\kappa_R = 0.5$, however in panel (b), where self-preservation is emphasised, the critical value is even less than that used for optimisation. We note that these are significantly less than the actual value of lethality for the Blue force; the optimisation is robust against variation in adversary lethality. In both cases, the threshold lethality is *insensitive* to the manoeuvre rate γ_R.

The exception to this insensitivity is at low γ_R for panel (a) where $\lambda = 0.5$: here the Blue force has an advantage for $\gamma_R \leq 0.5$ unless the Red force increases its lethality κ_R. Contrastingly, in panel (b) the Red force maintains advantage for $\kappa_R \geq 0.25$, right down to very small values of γ_R. Recalling the key result from our previous analyses, when offence is more valued in utility for $\lambda \leq 0.7$, the optimised Red networks strongly figure sacrificer nodes as a key mechanism in the engagement structure. As we saw in previous analyses, for $\lambda > 0.7$, these disappear and are replaced by Red manoeuvre hubs while all the remaining Red nodes engage with a small number of Blue. Thus in Fig.8(a), the optimised network will have more emphasis on attack rather than manoeuvre, with this flipping for panel (b). It is clear then that for (a), at low γ_R the optimised manoeuvre network is insufficient to guarantee victory - additional lethality is required. Contrastingly, in (b) the *manoeuvre* network gains prominence in the optimisation through the manifestation of hubs while the rest of Red are engaged in concentrating attacks on Blue. Thus *fewer* Red require to manoeuvre (they purely attack) *except through an efficient structure*, a hub. This leads to low γ_R values being sufficient for effectiveness against the Blue force.

Comparing Figs.8(a,b) we also see that in the region where Red does have advantage it scores *better* when *equally* weighting offence and defence (panel (a)) compared to emphasis on defence (in (b)). This seems in apparent contradiction to Fig.6(b) where at high λ the number of surviving Red forces is larger than at lower λ. However, at lower λ *no* Blue forces survive, unlike the case for larger λ. Thus the *difference* between steady-state force numbers at $\lambda = 0.9$ may indeed be less than for $\lambda = 0.5$.

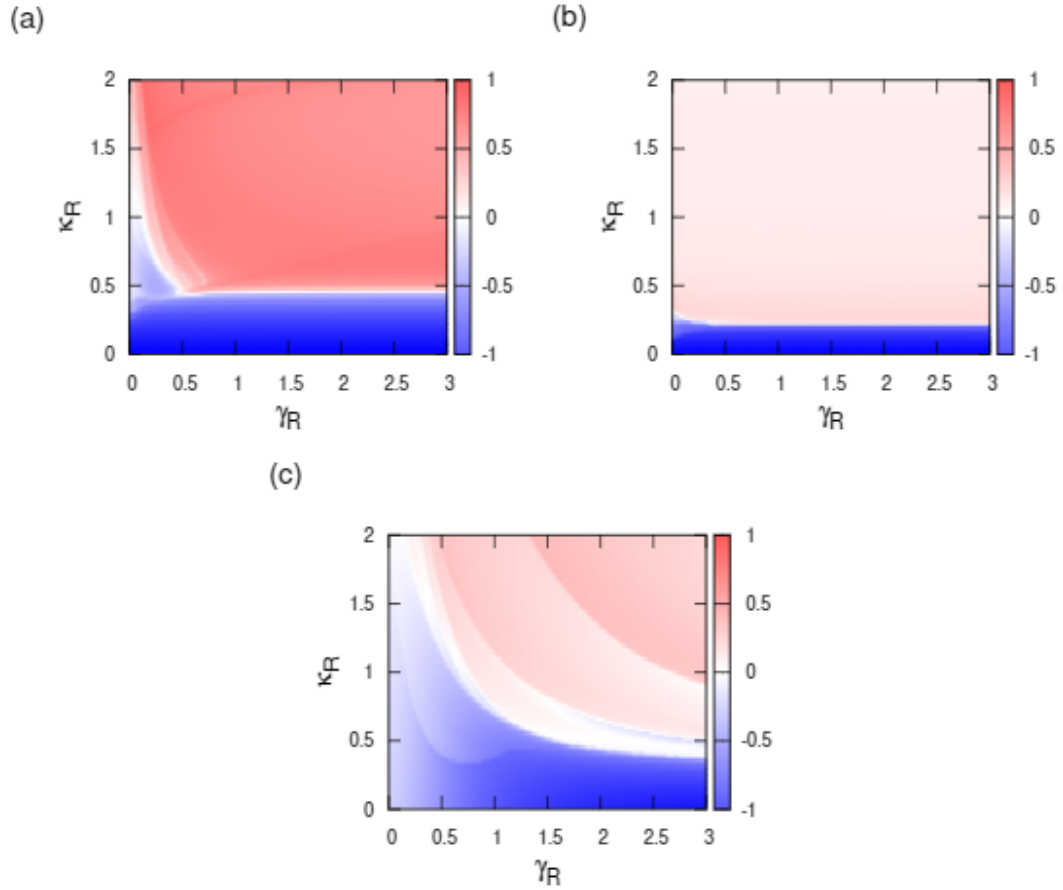In Fig.8(c) we show the result using the original random networks that seeded the

Figure 8. Plots of the victory heat-map showing the difference of steady-state densities for Red against Blue across values of γ_R, κ_R for $N_B = N_R = 50, L_B = L_R = 100$, and networks optimised for $\kappa_R = 0.5, \gamma_R = 1, \kappa_B = 1, \gamma_B = 1$ but solving the system for $\kappa_B = 3$. Panel (a) for $\lambda = 0.5$, (b) for $\lambda = 0.9$, and (c) the result using the original random network that seeded the optimisation.

optimisation; both Red and Blue have Erdos-Renyi random graphs. The shape of the cross-over region is understandable: Red has advantage when it is high in manoeuvre rate γ_R and fire-power κ_R. Contrasting this with the optimised results, we see the sensitivity in both of Red's parameters with gradients even beyond the threshold for Red victory. Thus the key role of optimisation is in flattening the variability in the various parameters.

To summarise these results, we see that with the capacity to invest in optimised networks, and fire-power or speed of manoeuvre through its structures, the Red force gains advantage through allocation of resources *up to a minimum level in fire-power*. Beyond that, it is wasted resource. Similarly, as long as it has optimised structure for both manoeuvre and engagement, the force only needs a minimal threshold in manoeuvre rate to gain advantage.

6.   Conclusions and Discussion

We have generalised the (N, M) Lanchester model to include manoeuvre warfare through the incorporation of networks. The model allows the embedding of warfighting heuristics for how a force dynamically redistributes resources through battle according to some local weighting across connections; here we used the local ratio of a force element to its adversaries. We optimised the structure of networked forces for both manoeuvre and engagement against a randomly structured adversary, as functions of an offence-defence trade-off and fire-power. We found consistently, that a force with optimised networks could defeat an equally sized opponent for lesser fire-power than that of the adversary. Depending on how it valued the offence-defence trade-off, different structures emerged for the optimised force.

We now reflect on how these structures figure in the literature of Manoeuvre Warfare.

Arguably, our model only narrowly reflects the manoeuvre dimension of warfare, purely in terms of the movement of resources around a networked force rather than the decision process. For something that is defined as *one* of the warfighting functions, military writings on Manoeuvre Theory tend to wrap numerous functions together, as well as the psychological dimensions of surprise and shock. Thus (Lind, 1985) draws upon the Manoeuvre Theory of John Boyd which treats Manoeuvre as a competition between adversarial Observe-Orient-Decide-Act (OODA) loops, itself a a model for C2. Thus our the manoeuvre rate constant γ is a proxy for the speed of each agent's OODA loop in the absence of an explicit structure for distributed decision making (also enabled by networks) that may facilitate or undermine the capacity to manoeuvre. In this interpretation, γ measures not just technology (speed and agility of vehicles or computers) but cognitive and psychological capacity.

Many authors see Sun Tzu (Smith and LeBrun, 1994) as the father of Manoeuvre Theory in his maxim "To subdue the enemy without fighting" (III.6). Clearly in our model, fighting is continuous through the process represented by the differential equations. However, implementations of Manoeuvre Theory into US Army doctrine, such as the 1970-1990s US Defense Reformers who emphasised (some argue, erroneously (Lauer, 1991)) "smaller, more mobile forces" against larger adversaries, *preserving one's own overall resource during the fight* is the real point of Sun Tzu. This our model captures and leads to recognisable structures. To this end we may focus on Clausewitz's *Principles of War* (Clausewitz, 1942), the tactical precursor to his most well-known work *On War* (Clausewitz, 1976): "We must select for our attack one

point of the enemy's position and attack it with great superiority, leaving the rest of his army in uncertainty but keeping it occupied. This is the only way that we can use an equal or smaller force to fight with advantage and thus with a chance of success. The weaker we are, the fewer troops we should use to keep the enemy occupied at unimportant points, in order to be as strong as possible at the decisive point." (Sect II.2.1). There follows a set of diagrams outlining how reserves may be used in certain tactical configurations, with forces circling an enemy and reserves in interior lines.

Though often contrasted with Sun Tzu as an attritionist, one can recognise here that Clausewitz espouses mobility of weaker forces to achieve *localised concentration* on the enemy. While valuing decisive battle over Sun Tzu's elusive force, Clausewitz emphasise manoeuvre in getting to that fight.

Analysing these ideas in reverse we see first in the manoeuvre hubs arising in the model for $\lambda \approx 1$ a pattern of how reserves should flow into battle, abstracted from spatial location, identifiable with Clausewitz's "formation in depth". The sacrificial nodes that emerged in the intermediate region of the offence-defence trade-off λ may be interpreted as *feints* – "unimportant points" – insofar as they distract the adversary fire with 'mass scale expendable' resources. These may be 'dummy' units, as we alluded in the introduction, which are replete in military history. Successful feints are based on incomplete information - the enemy lacks knowledge of the true nature of these targets. In our model the lack of information is reflected in the fact that engagement targets (of Red, from the Blue force) are assigned non-adaptively; only the manoeuvre of resource given the state of the fight is adaptive. If we were to use more sophisticated adaptive engagement mechanisms, such as examined by (MacKay, 2009) we can anticipate that this will change. The ignorance implied for such an interpretation of the sacrificial node behaviour is consistent with the absence of a representation of ISR at this stage of the model development.

The point of concentration of fire on the enemy is often described as the *schwerpunkt*. In our analyses, Blue is not optimised and thus is not adaptive to form structural or spatial hubs, thus offering Red a functional *schwerpunkt* for its attacks. The force with optimised networks thus attacks the ability of its adversary to manoeuvre resources, particularly when the number of attacks is constrained (as in the supplement), through what may be interpreted as *suppressive fires*. Finally, we may recognise in the collocation of manoeuvre and engagement hubs for the optimised force qualities seen in the coincidence of armour, speed, fire-power and mobile communications of the *panzer* divisions from 1940-41 of World War II. Indeed, this form of warfare was the realisation of many of the visions of manoeuvrist theorists, both British and German included, in the aftermath of the Great War.

These are qualitative observations about the patterns emerging in this mathematical approach. As alluded from the outset, the value of this approach is that it may be readily generalised further to include alternate heuristics for resource and target reallocation, and further warfighting functions. In particular, current work is developing this model to incorporate C2 through models of synchronising dynamical processes on network, effectively modelling the interactions of multiple Boyd OODA loops in the elements of each force. Logistics, built on yet other networks, are also straightforwardly incorporated into the model as source terms to represent how forces enter into and sustained through the battle. Also, using various differential equation based models of swarming, spatially embedding the model is also straightforward. It would be at this stage that appropriate validation studies should be undertaken to compare with data from a range of manoeuvrist centric battles in history. Nevertheless, we would agree with MacKay that the value of such models is less to be predictive (for

which the quality of data is often lacking), but more to explore more sophisticated warfighting concepts such as the role of, and balance of investments, across competing technologies, doctrine and human training to realise the various warfighting functions.

Acknowledgements

References

D.S. Alberts, J.J. Garstka, F.P. Stein. 1999. *Network Centric Warfare*. Washington DC, USA: Command and Control Research Program.

Albert, R., Barabasi, A.-L. 2002. "Statistical Mechanics of Complex Networks" *Rev.Mod.Phys.* 74, 47-97.

Boccaletti, S., et al. 2014. "The structure and dynamics of multilayer networks." *Physics Reports*, 544, 1-122.

Bornholdt, S., and Schuster, H.G. 2003. *Handbook of Graphs and Networks: From the Genome to the Internet*. New York, NY, USA: John Wiley and Sons, Inc.

Chuter, A. 2019. "The UK is ready to kick off an effort to revamp military training", Defense News, October 16.

Clausewitz, Carl von., Gatzke, Hans W. 1942. *Principles of War*. Harrisburg, PA., USA: The Military Service Publishing Company.

Clausewitz, Carl von., Howard, Michael. and Paret, Peter. 1976. *On War*. Princeton, N.J. USA: Princeton University Press.

Cole, R. 2019. "The Myths of Traditional Warfare: How Our Peer and Near-Peer Adversaries Plan to Fight Using Irregular Warfare", Small Wars Journal, Small Wars Foundation, Maryland, USA

Colegrave, R.K. and Hyde, J.M. 1993. "The Lanchester square-law model extended to a $(2, 2)$ conflict." *IMA J ApplMath* 51: 95-–109.

Epstein, J.M. 1997. "Nonlinear Dynamics, Mathematical Biology, and Social Science." Lecture Notes, Vol. 4, Santa Fe Institute Studies in the Sciences of Complexity. Reading, MA: Addison-Wesley.

Hohzaki, R. Higashio, T. 2016. "An attrition game on a network ruled by Lanchester's square law." *J Opl Res Soc* 67, 691–707.

Kaup, G.T., Kaup, D.J., Finkelstein, N.M. 2005. "The Lanchester $(n, 1)$ problem." *J Opl Res Soc* 56: 1399–1407.

Keane, T. 2011. "Combat modelling with partial differential equations." *App. Math. Model* 35, 2723–2735.

Kim, D., Moon, H., Park, D., Shin, H. 2017. "An efficient approximate solution for stochastic Lanchester models." *J Opl Res Soc* 68, 1470–1481.

Lanchester, F.W. 1916. *Aircraft in Warfare: the Dawn of the Fourth Arm*. London: Constable.

Lauer, G.S. 1991. "Maneuver Warfare Theory: Creating A Tactically Unbalanced Fleet Marine Force?" School of Advanced Military Studies, US Marine Corps, Fort Leavenworth: USA.

Lind, W.S. 1985. *Maneuver Warfare Handbook*. Westview Press: USA.

Liu, P.L., Sun, H.K., and You, Y.T. 2012. "Some comments on MacKay's Lanchester mixed forces model." Journal of the Operational Research Society, 63:11, 1631-1633.

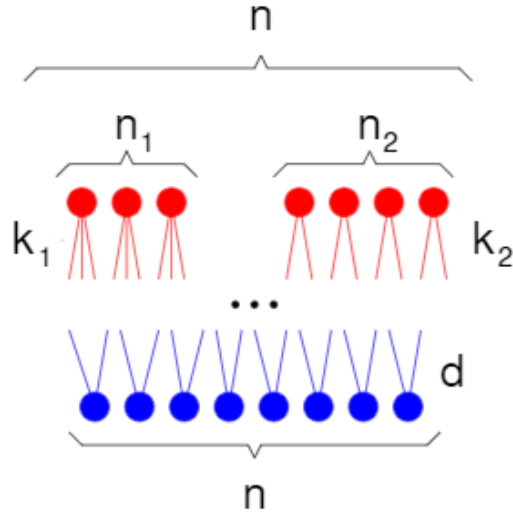Liu, J.X., Zhao, D.M., and Wang, F. 2013. "Networks attacks-defense model based on the im-

Figure 9. Illustration of a red force of n nodes comprised of two subgroups of size n_1 and n_2 who, respectively, each carry out k_1 and k_2 attacks on a blue force of size n, assuming that each blue node is attacked by d red nodes.

proved Lanchester equation." Proceedings of the 2013 International Conference on Machine Learning and Cybernetics, Tianjin, 14-17 July.

MacKay, N.J. 2009. "Lanchester models for mixed forces with semi-dynamical target allocation." *J Opl Res Soc* 60: 1421–1427.

MacKay, N.J. 2012. "Response to 'Some comments on MacKay's Lanchester mixed forces model.'" Journal of the Operational Research Society, 63:11, 1633.

McChrystal, S.A. 2011, "It takes a network." *Foreign Policy*, February 21.

Protopopescu, V., Santoro, R.T., and Dockery, J. 1989. "Combat modeling with partial differential equations." *Eur. J. Op. Res.* 38, 178–183.

Roberts, D.M. and Conolly, B.W. 1992. "An extension of the Lanchester square law to inhomogeneous forces, with an application to force allocation methodology." *J Opl Res Soc* 43: 741—752.

Roman, S. and Bullock, S. and Brede, M. 2017. "Coupled societies are more robust against collapse: a hypothetical look at Easter Island". *Ecological Economics*, 132: 264–278. (doi:10.1016/j.ecolecon.2016.11.003).

Smith, N D, and Nancy LeBrun. 1994. *S*un-tzu: Art of War. Bathesda, MD: Discovery Communications, Inc.

Tang, H., Li, Z.. 2012. "The phased Lanchester equations based on Network Centric Warfare", IEEE Fifth International Conference on Advanced Computational Intelligence(ICACI) October 18-20, 2012 Nanjing, Jiangsu, China.

US Army, 2017. Field Manual FM 3-0 Operations, Department of the Army, Washington DC

Appendix: An analytical explanation of 'sacrificer' nodes

In subsection 5.3, we saw that when optimising the combined engagement-manoeuvre networks a regime for low λ exists in which optimal configurations show the coexistence of 'normal' Red nodes that attack one Blue node each and a certain number of 'sacrificial' Red nodes which typically attack many Blue nodes, but don't receive support via the Red manoeuvre network. Here, we will show analytically that such nodes are indeed typical in our present setup, even without the presence of manoeuvre

support. Consider the set-up depicted in Fig. 9, in which the Red force composed of n nodes consists of two groups $n_1 + n_2 = n$ and fights a Blue adversary force made up of n nodes. Suppose, Red nodes in group one each attack k_1 Blue nodes and Red nodes in group two each attack k_2 nodes. Below, we will argue about parameters k_1, k_2, n_1, and n_2 that optimise outcomes for Red. For simplicity, we will further assume that Red nodes target Blue nodes at random. As there is a total of $L = L_1 + L_2 = n_1 k_1 + n_2 k_2$ attacks from the Red force, on average a Blue node will be targeted by $d = L/n$ Red nodes. Of these attacks, L_1/L are attacks from group one, and L_2/L attacks from group two. Overall, treating all Red nodes within a group and Blue nodes each as an average representative node, we thus arrive at the following system of equations governing the 'mean-field' Lanchester dynamics

$$\dot{R}_1 = -\kappa_B k_1 B \frac{n}{L} \tag{11}$$

$$\dot{R}_2 = -\kappa_B k_2 B \frac{n}{L} \tag{12}$$

$$\dot{B} = -\kappa_R \frac{L_1}{n} \frac{1}{k_1} R_1 - \kappa_R \frac{L_2}{n} \frac{1}{k_2} R_2, \tag{13}$$

where R_1 (R_2) is the force at an average group one (group two) Red node, and B the force of an average Blue node. Respectively multiplying Eqs. (11) and (12) by $-\kappa_R L(L_1/n^2)(R_1/k_1^2)$ and $-\kappa_R L(L_2/n^2)(R_2/k_2^2)$ and Eq. (13) by $\kappa_B B$ gives

$$\frac{d}{dt}\left(-\kappa_R \frac{L}{n^2}\left(\frac{n_1}{k_1}R_1^2 + \frac{n_2}{k_2}R_2^2\right) + \kappa_B B^2\right) = 0, \tag{14}$$

and we have thus found a typical invariant for the Lanchester dynamics. Suppose that, as also in our computational experiments, initial allocations of Blue and Red forces are equal. Then, in order to maximize battle outcomes for Red, the Red commander has to maximize the function

$$f(k_1, k_2, n_1) = \frac{L}{n^2}\left(\frac{n_1}{k_1} + \frac{n_2}{k_2}\right), \tag{15}$$

where $n_2 = n - n_1 \geq 0$. Straightforward analysis then shows that f is maximized for $n_1 = n/2$ and $k_1 = 1$ and $k_2 = n$ (or $k_1 = n$, $k_2 = 1$). Consequently, optimal results for Red are achieved if Red splits its force into one group of nodes that each attack all Blue nodes and one group of nodes who each attack exactly one Blue node, namely if Red diverts a substantial amount of its forces as sacrificial nodes.

The advantage Red can gain by introducing sacrificial nodes is seen when we evaluate comparable invariants of the Lanchester dynamics. We find the following victory conditions for Red. Presuming that each Red node initially has equal force $R_1(t = 0) = R_2(t = 0) = R_0$ and $B(t = 0) = B_0$, at the optimal engagement configuration we have

$$\kappa_R R_0^2\left(\frac{1}{2} + \frac{n}{4} + \frac{1}{4n}\right) > \kappa_B B_0^2, \tag{16}$$

whereas for a non-optimised engagement in which $k = k_1 = k_2$ one has

$$\kappa_R R_0^2 > \kappa_B B_0^2. \tag{17}$$

24

Thus, in the limit of very large forces $n \gg 1$ a Red commander who optimises its engagement structure only needs to bring a fraction $2/\sqrt{n}$ of the force to gain victory compared to the non-optimised configuration.